Abcc10 status affects mammary tumour growth, metastasis, and docetaxel treatment response

N Domanitskaya[1], J Wangari-Talbot[1], J Jacobs[1], E Peiffer[1], Y Mahdaviyeh[1], C Paulose[1], E Malofeeva[1], K Foster[1], K Q Cai[1], Y Zhou[1], B Egleston[1] and E Hopper-Borge*,[1]

[1]Program in Developmental Therapeutics, Fox Chase Cancer Center, Philadelphia 19111, PA, USA

Background: Resistance to chemotherapeutic agents is a major obstacle to cancer treatment. A group of ABC efflux pumps, the Multidrug Resistance Proteins, is a source of resistance. Herein, we investigated the role of ABCC10 in mammary tumours, given the important role we have defined for ABCC10 in transporting taxanes, and the recognition that some ABCC proteins have roles in tumour growth.

Methods: ABCC10 expression was correlated to human breast cancer subtype using breast tissue microarrays. Real-time quantitative PCR and western blot analysis were used to examine ABCC10 expression in human breast cancer lines. $Abcc10^{-/-}$ mice were crossed to MMTV-PyVmT mice to produce $Abcc10^{-/-}$ vs $Abcc10^{+/+}$ mammary tumours and derivative cell lines. We used allograft and cellular assays to perform baseline and drug sensitization analysis of tumours and cell lines.

Results: Clinical sample analyses indicated that ABCC10 was more highly expressed in Her2+ and ER+ than in Her2−, ER−, and triple-negative breast cancer. Unexpectedly, PyVmT; $Abcc10^{-/-}$ tumours grew more rapidly than PyVmT; $Abcc10^{+/+}$ tumours and were associated with significantly reduced apoptosis and metastasis. PyVmT; $Abcc10^{-/-}$ lines were less migratory than PyVmT; $Abcc10^{+/+}$ lines. Finally, we showed increased survival of docetaxel-treated MMTV-PyVmT; $Abcc10^{-/-}$ mice compared with wild-type mice.

Conclusions: These data identify roles for Abcc10 in breast cancer pathogenesis and in vivo docetaxel resistance.

Much of the mortality of any cancer is associated with resistance to therapeutic agents. Docetaxel and paclitaxel have been mainstays of breast cancer treatment regimens and the development of chemotherapeutic resistance to these agents has long been a major impediment to cancer treatment. One reported contributing factor to multidrug resistance is the overexpression of a class of efflux pumps known as ATP-Binding Cassette (ABC) transporters. The C subfamily of ABC proteins, alternatively known as the ABCC proteins, or the Multidrug Resistance Protein subfamily, consists of nine family members. These pumps confer resistance to and transport several classes of chemotherapeutics including taxanes, vinca alkaloids, and anthracyclines, as well as physiological substrates including leukotrienes (Glavinas et al, 2004; Keppler, 2011).

Taxanes are important agents in the treatment of many cancers, including breast cancer (Woodward and Twelves, 2010). Well-studied taxane pumps such as ABCB1 have been highly investigated over the past few decades as possible mediators of taxane resistance in breast cancer. To date, numerous studies have been unable to find a clinical benefit of inhibiting ABCB1 (Kelly et al, 2012; Amiri-Kordestani et al, 2013).

By contrast, although we and others have demonstrated that ABCC10 expression is widespread (Hopper et al, 2001; Wang et al, 2009), few studies have addressed the role of this protein in in vivo treatment resistance. ABCC10 is a particularly interesting transporter to study, as overexpression of ABCC10 in vitro confers resistance to an unusually wide range of clinically valuable drugs,

BJC OPEN

including taxanes, vinca alkaloids, nucleoside analogues, and epothilone B (Hopper-Borge et al, 2004; Oguri et al, 2008; Hopper-Borge et al, 2009). Excitingly, we used a newly developed $Abcc10^{-/-}$ mouse model to show that absence of this transporter in vivo sensitises animals to taxanes, with $Abcc10^{-/-}$ mice experiencing increased sensitivity (that is, increased neutropenia and bone marrow hypoplasia) compared with their wild-type counterparts following paclitaxel treatment (Hopper-Borge et al, 2011). These findings also suggest that modulation of ABCC10 activity by inhibitors may have clinical value in management of breast cancer and other cancers that are treated with taxanes, based on action in eliminating these drugs from breast tumour tissue.

Besides direct action in regulating drug efflux, a growing and intriguing body of work suggests that some ABC transporters may affect cancer biology in additional ways that affect disease course or treatment. A recent study has implied a link between ABCC1, ABCC11, and poor prognosis in breast cancer (Yamada et al, 2013). ABCC1, ABCC3, and ABCC4 have clinical and biological effects in neuroblastoma independent of their abilities to efflux drug (Henderson et al, 2011). For all of these transporters, expression tends to increase with age, causing them to be more abundant at the time of great rates of cancer onset. Interestingly, ABCC1 suppresses neuroblastoma development in an hMCYN mouse model. In vitro inhibition of ABCC1 and ABCC4 suppresses wound closure, whereas ABCC3 overexpression inhibits cell migration and cell line clonogenicity (Henderson et al, 2011). Such unexpected activities might also affect drug resistance, by affecting the proliferation rate of tumours, or by contributing to epithelial–mesenchymal transitions that are associated with general drug resistance (Dave et al, 2012; McMillin et al, 2013).

To date, few studies have addressed the impact of ABCC10 in breast cancer. One recent study showed that ABCC10 mRNA is upregulated in breast carcinoma and that its expression correlates with ER status (Hlavac et al, 2013). We have now examined the expression of the ABCC10 protein in breast tumours and breast cancer cell lines to establish physiological relevance in this context. To further investigate the role of ABCC10 in breast cancer, and in particular the viability of ABCC10 as a target for cancer treatment, we have also bred $Abcc10^{-/-}$ mice to the well-described mouse mammary tumour virus-polyomavirus middle T (MMTV-PyVmT) model (Lin et al, 2003). We chose this model because detailed pathological analysis of PyVmT tumours indicates that the progression from premalignant to highly malignant stages is very similar to that seen in human breast tumours (Lin et al, 2003). Together, our data showed for the first time that ABCC10 affects multiple parameters of breast tumour biology and may modulate the efficacy of docetaxel to treat tumours.

MATERIALS AND METHODS

Cell lines. HS578T, BT549, T47D, MDA-MB-231 human breast cancer cell lines were purchased from the National Cancer Institute (Bethesda, MD, USA). MCF10F, MCF7, BT474, SKBR-3, MDA-MB-361 human breast cancer cell lines were purchased from the American Type Culture Collection (ATCC). Cells were passaged in our laboratory for fewer than 3 months after receipt or resuscitation.

Reagents. [^{3}H]-docetaxel (5 Ci mmol^{-1}; Moravek Biochemicals Inc, Brea, CA, USA). Docetaxel was purchased from LC Laboratories (Woburn, MA, USA). Paclitaxel was purchased from Sigma (St Louis, MO, USA).

Mouse strains, handling and measurement of tumours. All experiments involving mice were preapproved by the Fox Chase Cancer Center Institutional Animal Care and Use Committee. MMTV-PyVmT mice of the 634Mul/J subline were purchased

from The Jackson Laboratory (Bar Harbor, ME, USA). Homozygous $Abcc10^{-/-}$ mice (Hopper-Borge et al, 2011) were crossed with MMTV-PyVmT mice to generate the $Abcc10^{-/-}$; PyVmT-positive and $Abcc10^{+/+}$ PyVmT-positive female siblings for analysis. We have confirmed that Abcc10 is lost in this model at the RNA and protein levels. Tumour volumes were calculated following caliper measurement as width$^2 \times$ length $\times$ 0.52. Mice were killed by methoxyfluorane inhalation when the tumours reached 10% of mice body weight or if mice exhibited signs of illness or distress.

Xenograft studies. MMTV-PyVT;$Abcc10^{+/+}$ and MMTV-PyVT;$Abcc10^{-/-}$ mammary tumour-derived cells were implanted into the mammary gland area of 8-week-old female SCID mice ($n = 15$ per cell line). Two weeks later, when the tumours grew to ~ 50 mm^3, the mice were divided into two groups: vehicle ($n = 5$) and 25 mg kg^{-1} docetaxel treatment ($n = 10$). To evaluate tumours, a very dense measuring technique was used to assess solid tumour mass and to reduce the volume added from liquid. The mice were treated weekly by intraperitoneal injection until the tumours reached the maximum size (200 mm^3); at the end of the experiment mice were killed by methoxyfluorane inhalation.

Immunohistochemical analysis. The largest tumour and lungs were excised, divided, and fixed 24–48 h in 10% neutral-buffered formalin. Specimens were paraffin-embedded, sectioned, and analysed with haematoxylin/eosin staining. Consecutive 5-μm sections were cut and mounted on silinized slides (Superfrost Plus, Fisher Scientific Inc., Waltham, MA, USA). Sections were deparaffinised in xylene and rehydrated in a graded series of ethanol. The sections were subjected to antigen retrieval by boiling in 0.01-M sodium citrate buffer (pH 6.0) in a steamer for 20 min and allowed to cool in the buffer for 20 min. Immunostaining was performed by standard protocols previously described (Cai et al, 2009). All slides were viewed with a Nikon Eclipse 50i microscope and photomicrographs were taken with an attached Nikon DS-Fi1 camera (Melville, NY, USA). Lung metastases were expressed as number of metastases per square millimetre of lung cross-section using Image Pro-Plus (Media Cybernetics, Silver Spring, MD, USA). Immunostained slides (for Ki-67) were scanned using an Aperio ScanScope CS 5 slide scanner (Aperio, Vista, CA, USA) with a $\times 40$ objective. Scanned images were then viewed with Aperio's image viewer software (ImageScope, version 11.1.2.760, Aperio). Selected regions of interest were outlined manually by a pathologist. Proliferative index (Ki-67) was quantified using Aperio Nuclear V9 algorithm (Aperio) with modifications.

Tissue microarray (TMA). A breast TMA was constructed as previously described (Kononen et al, 1998; Parsons, 2009). The intensity of immunostaining using a monoclonal ABCC10 antibody (Hopper-Borge et al, 2009) was scored visually by an experienced pathologist. For certain statistical analyses, absence of ABCC10 staining was considered to be one group and presence of ABCC10 staining was considered to be another group.

Derivation of mammary tumour cells and cellular assays. Cell lines were derived as previously described (Izumchenko et al, 2009). Drug accumulation assay was performed as previously described (Hopper-Borge et al, 2004). Proliferation was quantitated with CyQuant (Invitrogen, Eugene, OR, USA) according to the manufacturer's instructions and adhesion of cells was monitored by the xCELLigence Real-Time Cell Analysis detection platform (ACEA Bioscience Inc., San Diego, CA, USA). Cellular proliferation assays with HEK-293 cells were performed as previously described (Hopper-Borge et al, 2009). To analyse change of mammary tumours, cell line shape factor after drug treatment cells were stained for phalloidin-FITS-conjugated, 4',6-diamidino-2-phenylindole (DAPI) and Deep Red Cell Mask. Image quantitative analysis was performed with the MetaXpress 3.1 software

(MDS Analytical Technologies, Sunnyvale, CA, USA). Confocal laser scanning microscopy was performed as previously described (Malofeeva et al, 2012). Cell cycle and apoptosis analyses were assessed using Guava Nexin and cell cycle reagents (Guava Technologies, Hayward, CA, USA) according to the manufacturer's protocol. For all cytotoxicity experiments, treatment of Abcc10 knockout and wild-type cells was started after the cells were attached completely.

Colony formation and wound-healing assays. PyVmT; $Abcc10^{+/+}$ and PyVmT; $Abcc10^{-/-}$ mammary tumour cell lines were seeded at low density in individual wells of a standard six-well plate and treated with docetaxel or paclitaxel for 5 days. Colonies were visualised with crystal violet staining. For wound-healing assays, cell-free areas were generated with a pipette tip on a confluent monolayer. Cells were treated with docetaxel (3 nM) or paclitaxel (3 nM). Two or three wound areas per condition were photographed at 8 or 24 h. Wound size was quantified by measuring the cell-free areas using the Image-J software (NIH, Bethasda, MD, USA).

Quantitative real-time PCR. Total RNA was isolated using the RNeasy mini kit (Qiagen, Valencia, CA, USA) according to the manufacturer's suggestions. RNA was reverse-transcribed using the M-MLV reverse transcriptase and a mixture of anchored oligo-dT primers and random decamers. Aliquots of cDNA were used for qRT–PCR. Cycling conditions were 95 °C, 15 min followed by 40 cycles (95 °C, 15 s; 60 °C, 60 s). To compare transporter expression levels, all mean quantity data were normalised to an independent gene Ppib (cyclophilin B).

Western blot analysis. Western blot analysis was performed as described (Izumchenko et al, 2009). Anti-Abcc10 antibody was used at a concentration of 1:500 (Hopper-Borge et al, 2011). ABCB1, ABCG2 (Santa Cruz Biotechnology, Dallas, TX, USA), β-actin (Abcam, Cambridge, MA, USA), HER2 and ERα (Cell Signalling Technology, Danvers, MA, USA) antibodies were used according to the manufacturer's instructions.

Statistical procedures. We used Fisher's exact tests for Figure 1C. We used Kaplan–Meier curves with log-rank tests for Figures 2A and 7C. We used generalised linear models estimated by generalised estimating equations with appropriate working correlation matrices for Figures 2B, 6A, 7A and B (Shults et al, 2007). We used restricted cubic splines to model day effects where there were enough days to do so (Harrell, 2001). The previous analyses were conducted using STATA (StataCorp, College Station, TX, USA). For Supplementary Figure 1 data from two data sets were background-corrected and RMA-normalised (Bolstad et al, 2003), then LIMMA methodology (Smyth, 2004) was applied to conduct the differential analysis between tumour and normal tissues. For other analyses, we used two-sided Student's t-tests. Error bars in figures represent one s.e. intervals, unless otherwise noted. The nominal criteria for statistical significance was set to $P < 0.05$.

RESULTS

Elevated ABCC10 protein expression in human HER2+ and ER+ breast cancer. A prior study examined ABCC10 expression at the mRNA level using the NCI panel cell lines (Szakacs et al, 2004). As a way to ascertain the ABCC10 protein expression levels in breast cancer, we examined eight well-characterised breast cancer-derived cell lines and one nontumorigenic breast epithelial cell line as a control. Other groups have previously shown that HER2 and ER expression positively correlates with taxane resistance (Ueno et al, 1997; Sui et al, 2007) and we decided to analyse the expression of ABCC10 in the context of ER and HER2 status of the cell lines. We determined that ABCC10 was expressed in all cell lines and was expressed most highly in MCF7, T47D, and

BT474 cell lines (Figure 1A). In contrast, HS578T, BT549, and MDA-MB-231, all triple-negative cell lines expressed the lowest levels of ABCC10. Upon further analysis, we determined that ABCC10 expression was higher in HER2-positive cell lines compared with HER2-negative cell lines (Figure 1B and Supplementary Figure 1). However, greater significance was observed in the ABCC10 expression levels of ER-positive lines compared with ER-negative lines (Figure 1B and Supplementary Figure 1). We also analysed ABCC10 mRNA level in two breast cancer data sets from Gene Expression Omnibus (GSE5764 and GSE8977). ABCC10 expression was significantly higher in tumour than in normal lobular breast tissue in contrast to ABCB1 and ABCG2 expression (Supplementary Figure 2). We developed and screened TMAs containing 51 (Figure 1C and D) breast cancer specimens, including 18 HER2+, 15 HER2−, and 18 triple-negative (ER−/PgR−/HER2−) samples; we chose these breast cancer subtypes to focus on primarily because they are treated with chemotherapeutic agents that are ABCC10 substrates. We found that ABCC10 expression correlated positively with HER2+ and surprisingly ER+ status. In addition, using HEK-ABCC10 transfectants (Hopper-Borge et al, 2009) we found that ABCC10 did not confer cellular resistance to tamoxifen, the agent used primarily to treat ER+ breast cancer (Higgins and Baselga, 2011). In these standard proliferation assays ($n = 7$) we found the IC_{50} for the control cell line HEK-293 to be $187.5 \pm 23.6\,\mu M$ vs for the ABCC10 transfectant lines, $202 \pm 21.6\,\mu M$ for HEK-ABCC10-C17 and $190.4 \pm 26.0\,\mu M$ for HEK-ABCC10-C18. We observed that ABCC10 was expressed mainly in the cytoplasm and membrane. In addition, triple-negative breast cancer subtype showed higher heterogeneity for ABCC10 expression compared with other cancer subtypes (38.9% of ER−/PgR−/HER2− samples did not express ABCC10 vs 6.7% and 0% for HER2− and HER2+ breast cancer subtypes, respectively, Figure 1C). We also noted a tendency towards increased ABCC10 expression with age (Supplementary Table 1).

Mammary tumour growth is enhanced in MMTV-PyVmT;$Abcc10^{-/-}$ vs MMTV-PyVmT;$Abcc10^{+/+}$ mice. To understand the role of Abcc10 in mammary tumours in a physiological context, we bred $Abcc10^{-/-}$ mice (Hopper-Borge et al, 2011) to mice expressing the MMTV-PyVmT transgene. The MMTV-PyVmT mouse mammary model (Guy et al, 1992) has been used in numerous publications in the past (Forrester et al, 2005; Izumchenko et al, 2009; Marcotte et al, 2012; Ishihara et al, 2013). Latency until detection of mammary tumours was comparable in MMTV-PyVmT; $Abcc10^{-/-}$ and MMTV-PyVmT; $Abcc10^{+/+}$ mice (Figure 2A). Abcc10$^{+/+}$ status, however, significantly limited the total tumour burden of MMTV-PyVmT mice. After 20 weeks, tumours derived from MMTV-PyVmT; $Abcc10^{-/-}$ animals reached an average volume of 1000 mm^3, whereas tumours derived from MMTV-PyVmT; $Abcc10^{+/+}$ mice had an average volume of 300 mm^3 ($P = 0.020$; Figure 2B). Given this result, it was surprising that after killing, histopathological analysis revealed that MMTV-PyVmT; $Abcc10^{+/+}$ and MMTV-PyVmT; $Abcc10^{+/-}$ tumours were less differentiated than MMTV-PyVmT; $Abcc10^{-/-}$ tumours ($P = 0.030$; Supplementary Table 2), as less differentiated tumours are typically more aggressive, metastasise early, and have a much poorer prognosis (Soerjomataram et al, 2008). Quantification of blood vessel density with CD31 staining showed a trend towards higher vascularisation of MMTV-PyVmT; $Abcc10^{+/+}$ tumours, and Caspase 3 staining indicated a higher rate of apoptosis in wild-type tumours compared with Abcc10 null tumours (Figure 2C). Interestingly, increased Caspase 3 activity correlates with a worse prognosis (O'Donovan et al, 2003). Analysis of lungs from mice bearing primary mammary tumours indicated greater levels of metastasis in MMTV-PyVmT; $Abcc10^{+/+}$ tumours compared with MMTV-PyVmT; $Abcc10^{-/-}$ tumours (Figure 2D).
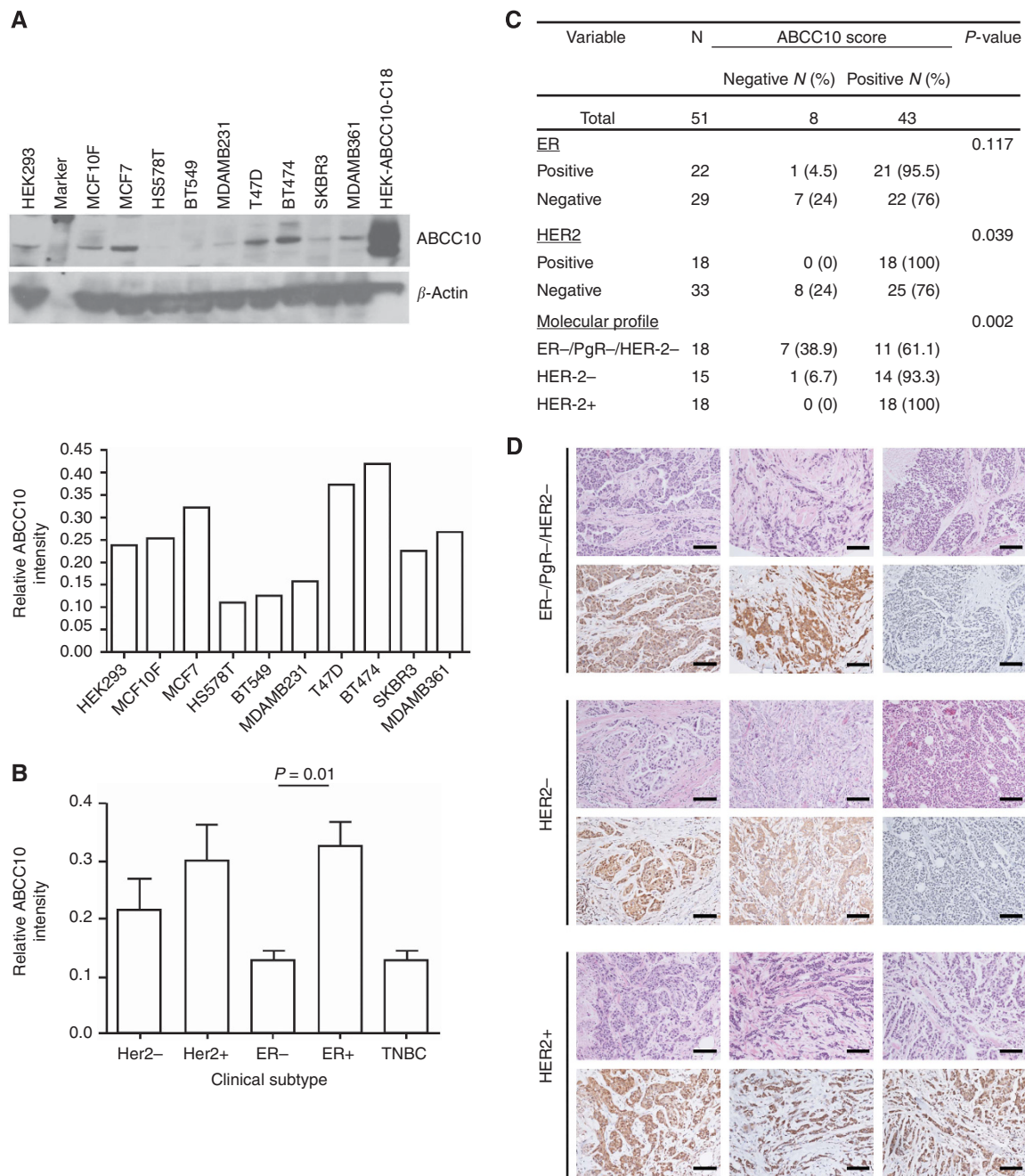
Variable	N	ABCC10 score		P-value
		Negative N (%)	Positive N (%)	
Total	51	8	43	
ER				0.117
Positive	22	1 (4.5)	21 (95.5)	
Negative	29	7 (24)	22 (76)	
HER2				0.039
Positive	18	0 (0)	18 (100)	
Negative	33	8 (24)	25 (76)	
Molecular profile				0.002
ER–/PgR–/HER-2–	18	7 (38.9)	11 (61.1)	
HER-2–	15	1 (6.7)	14 (93.3)	
HER-2+	18	0 (0)	18 (100)	

Figure 1. ABCC10 expression in human breast cancer cell line and primary tumours. (A) Top, western blot showing ABCC10 protein levels in nontumorigenic epithelial cell lines, HEK-293 and MCF10F, human breast cancer lines MCF7, HS578T, BT549, MDA-MB-231, T47D, BT474, SKBR-3, and MDA-MB-361. An ABCCC10-overexpressing HEK transfectant (HEK-ABCC10-C18) was used as a positive control. Bottom, relative ABCC10 expression from three separate blots. (B) ABCC10 expression in HER2− (MCF7, HS578T, BT549, MDA-MB-231, and T47D), HER2+ cell lines (BT474, SKBR-3, and MDA-MB-361), ER− (HS578T, BT549, MDA-MB-231, and SKBR-3) ER+ (MCF7, T47D, BT474, and MDA361), and triple-negative (TNBC) (HS578T, BT549, MDA-MB-231). (C, D) Correlation of ABCC10 expression with HER2 status, ER status, and with the triple-negative breast cancer subtype was determined using immunohistochemical analysis of 51 human breast tumours. Scale bar, 100 μm. Error bars denote mean ± s.e.m. Statistical significance was determined by two-sided Student's t-test.

Abcc10 status affects the growth of mammary tumour-derived cell lines. To better understand ABCC10-mediated effects on cancer progression and drug resistance, we derived MMTV-PyVmT; $Abcc10^{-/-}$ and MMTV-PyVmT; $Abcc10^{+/+}$ tumour cell lines (Figure 3A). We found that the rate of proliferation of MMTV-PyVmT; $Abcc10^{+/+}$ cells was initially comparable to that of MMTV-PyVmT; $Abcc10^{-/-}$ cells; however, 6 days after plating, MMTV-PyVmT; $Abcc10^{-/-}$ had an increased proliferation rate (Figure 3B). To ascertain whether adhesion had a role in

the growth rate differences between PyVmt;$Abcc10^{+/+}$ and PyVmT;$Abcc10^{-/-}$ mammary tumour-derived cell lines, we seeded cells and allowed attachment for 24 h. By 24 h all knockout cells attached, in contrast fewer Abcc10 wild-type cells were attached at this time point (Figure 3C). This result was confirmed by real-time monitoring of cell adhesion and spreading with xCELLigence system over a 24-h period (Figure 3D). A colony formation assay revealed that MMTV-PyVmT; $Abcc10^{-/-}$ cells formed threefold larger foci than MMTV-PyVmT; $Abcc10^{+/+}$
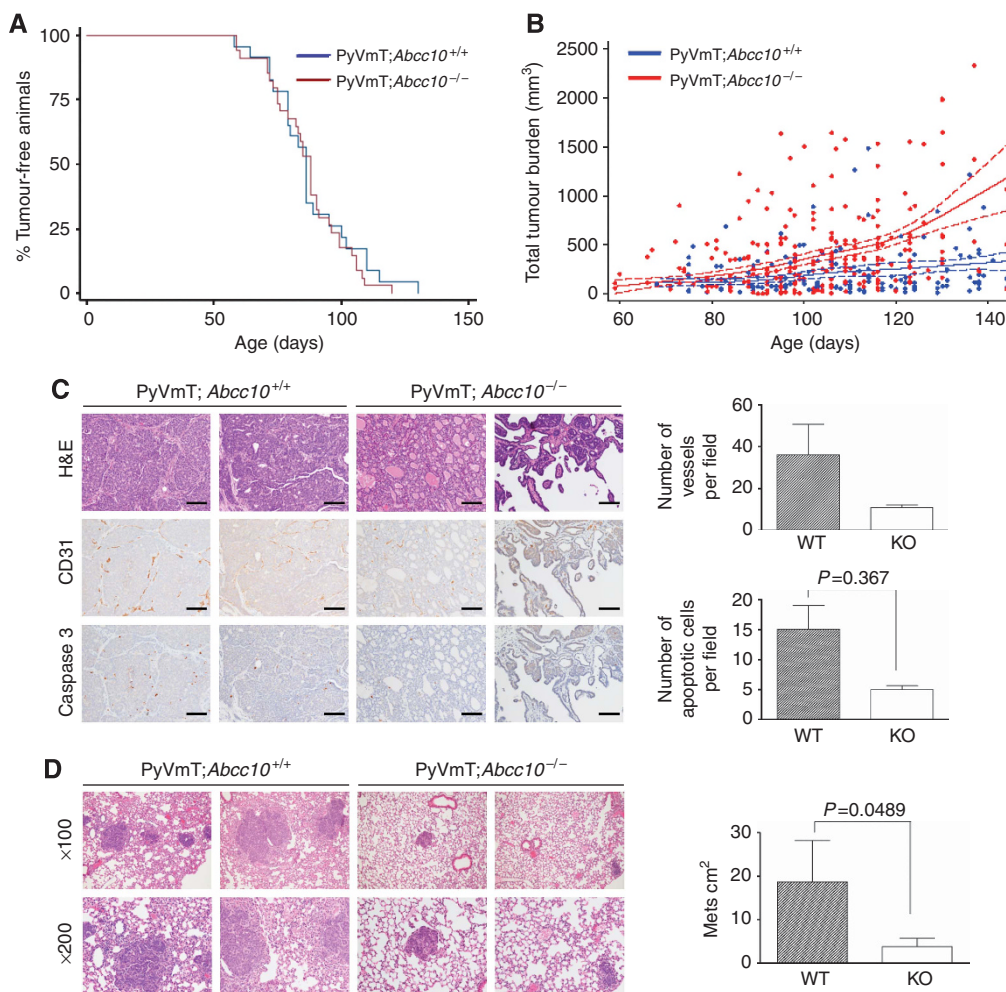
Figure 2. Tumour development in MMTV-PyVmT mice with Abcc10$^{-/-}$ and Abcc10$^{+/+}$ genotypes. (**A**) Kaplan–Meier curve analysis did not indicate significant differences in timing of tumor incidence in MMTV-PyVmT; Abcc10$^{-/-}$ (red line; $n = 26$) vs MMTV-PyVmT; Abcc10$^{+/+}$ (blue line; $n = 21$) mice. (**B**) Comparison of growth rates of MMTV-PyVmT; Abcc10$^{-/-}$ mammary tumours and MMTV-PyVmT; Abcc10$^{+/+}$ tumours. (**C**) H&E, CD31, and Caspase 3-stained sections of tumours isolated from MMTV-PyVmT;Abcc10$^{+/+}$ and MMTV-PyVmT; Abcc10$^{-/-}$ mice ($n = 5$ per genotype). Scale bar, 100 μm. (**D**) H&E-stained lung sections isolated from MMTV-PyVmT; Abcc10$^{+/+}$ and MMTV-PyVmT; Abcc10$^{-/-}$ mice. Error bars denote mean ± s.e.m. Statistical significance was determined by two-sided Student's t-test.

cells (Figure 3E). Further, MMTV-PyVmT; Abcc10$^{-/-}$ cells are significantly larger than MMTV-PyVmT; Abcc10$^{+/+}$ cells (Figure 3F). *Finally, a wound-healing assay was used to assess differences in migration of Abcc10 wild-type and null cell lines. We found that 24 h post scratch*, MMTV-PyVmT; Abcc10$^{-/-}$ cells migrated ∼40% less compared with MMTV-PyVmT; Abcc10$^{+/+}$ cells (Figure 3G).

We assessed whether other transporters were modulated as a result of Abcc10 loss. mRNA expression of Abcc1, Abcc3, Abcc4, Abcc5, Abcb1a/b, and Abcg2 was not elevated to compensate for Abcc10 loss (Supplementary Figure 3). Interestingly, there was a significant downregulation of Abcg2 in Abcc10$^{-/-}$ cell lines compared with Abcc10$^{+/+}$ cells (Figure 3H). However, a reduced level of Abcg2 in Abcc10$^{-/-}$ cell lines would likely not have an impact on taxane sensitization as the class of taxanes is not an abcg2 substrate (Huisman et al, 2005).

MMTV-PyVmT;Abcc10$^{-/-}$ mammary tumour cells are sensitised to taxanes. We used the well-established colony formation assay to assess taxane cytotoxicity on the primary tumour lines as previously described (Grassilli et al, 2013; Kuo et al, 2006). A 5-day treatment with 3 nM paclitaxel did not affect foci formation in MMTV-PyVmT; Abcc10$^{+/+}$ cell lines while decreasing formation by more than 20% in

MMTV-PyVmT; Abcc10$^{-/-}$ cell lines. Similarly, in MMTV-PyVmT; Abcc10$^{+/+}$ cells, treatment with 3 nM docetaxel produced 45% fewer colonies vs vehicle-treated cells but 90% fewer colonies in MMTV-PyVmT; Abcc10$^{-/-}$ cells (Figure 4A).

In addition, incubation with taxanes affected the morphology of Abcc10 null cells more dramatically than Abcc10 wild-type cells. Analysis of phalloidin, DAPI, Deep Red Cell Mask staining with a fluorescence microscopy showed a significant change in the cell shape factor of MMTV-PyVmT; Abcc10$^{-/-}$ cell lines after paclitaxel or docetaxel treatment (Supplementary Figure 4). Docetaxel is a microtubule-stabilizing agent: we observed significant tubulin stabilisation at 3 nM docetaxel in MMTV-PyVmT; Abcc10$^{-/-}$ cells, whereas MMTV-PyVmt;Abcc10$^{+/+}$ cells required a higher concentration (25 nM) for a similar effect (Figure 4B). We also examined the wound closure ability of the MMTV-PyVmt;Abcc10$^{+/+}$ compared with MMTV-PyVmt;Abcc10$^{-/-}$ cell lines after docetaxel treatment. We noted a more dramatic effect on cellular migratory activity of 3 nM docetaxel treatment on Abcc10-disrupted lines at 8 and 24 h post treatment (Figure 4C).

These genotype-associated differences are all compatible with the idea that higher effective concentrations of taxanes accumulate in MMTV-PyVmt;Abcc10$^{-/-}$ cell lines. We incubated mammary cell lines of both genotypes with 0.1 μM [^{3}H]-docetaxel in an
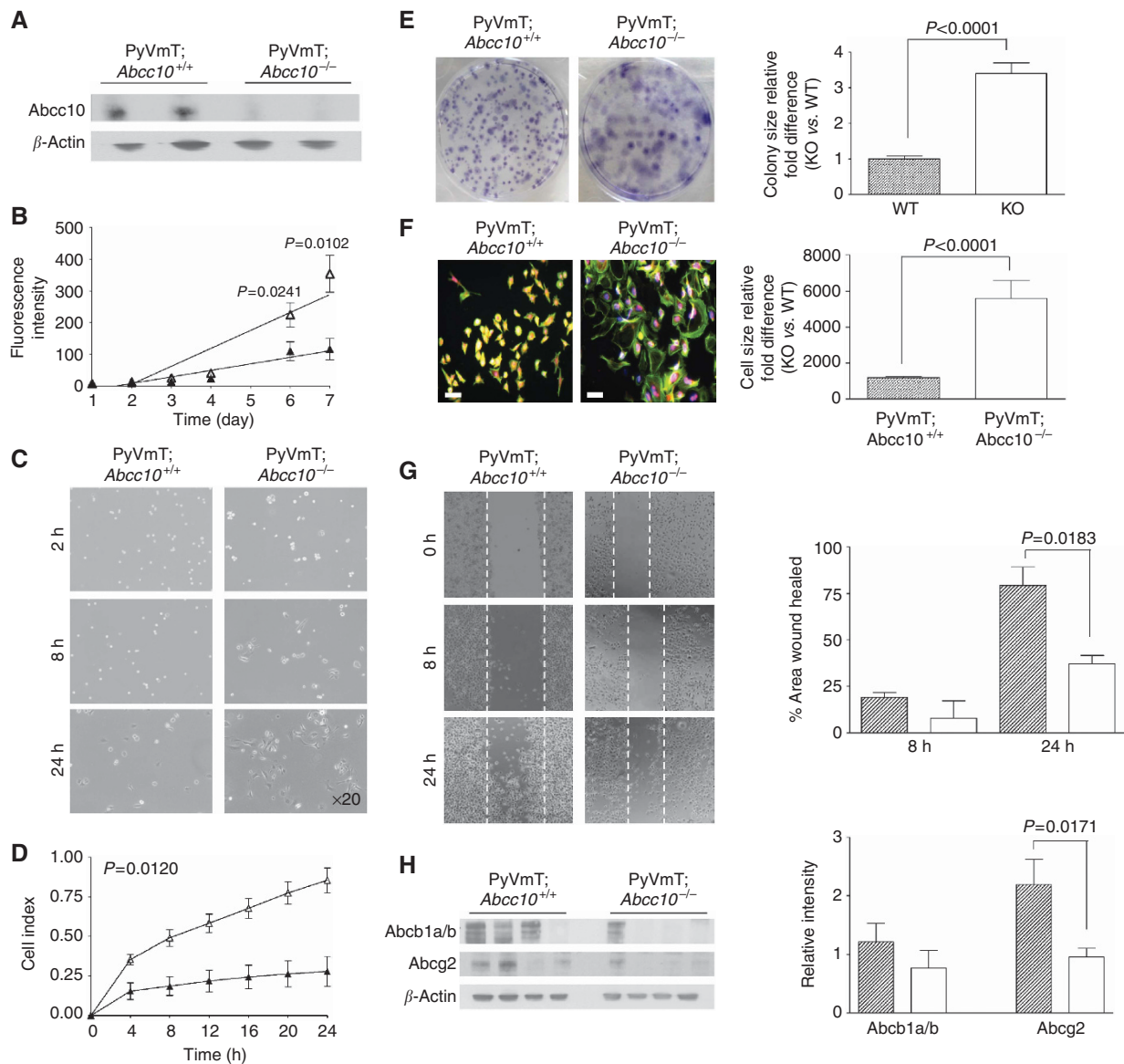
Figure 3. Characterisation of MMTV-PyVmT; *Abcc10*$^{+/+}$ and MMTV-PyVmT; *Abcc10*$^{-/-}$ mammary tumour-derived cell lines. (A) Abcc10 protein expression in MMTV-PyVmT; *Abcc10*$^{-/-}$ and MMTV-PyVmT; *Abcc10*$^{+/+}$ tumour cell lines. **(B)** CyQuant analysis of proliferation of wild-type (black triangle) and *Abcc10*$^{-/-}$ (white triangle) cell lines. **(C, D)** Comparison of the cell-adhesive abilities: *Abcc10* wild-type and null cell lines at times 0, 8, and 24 h after seeding, representative images of are shown **(C)**; monitoring of cell adhesion and spreading with xCELLigence system. MMTV-PyVmT; *Abcc10*$^{-/-}$ (open triangles) and MMTV-PyVmT; *Abcc10*$^{+/+}$ (closed triangles, shaded) **(D, E)** Images of colonies formed by MMTV-PyVmT; *Abcc10*$^{-/-}$ (open triangles) and MMTV-PyVmT; *Abcc10*$^{+/+}$ tumour cell lines. **(F)** Analysis of *Abcc10*$^{+/+}$ and *Abcc10*$^{-/-}$ cell size; phalloidin (green), nuclei (blue), and Deep Red Cell Mask (red). Scale bar, 50 μm. **(G)** Wound closure ability of MMTV-PyVmT; *Abcc10*$^{+/+}$ and MMTV-PyVmT; *Abcc10*$^{-/-}$ cell lines. **(H)** Abcb1a/b and Abcg2 protein expression in MMTV-PyVmT; *Abcc10*$^{-/-}$ and MMTV-PyVmT; *Abcc10*$^{+/+}$ tumour cell lines. Error bars denote mean ± s.e.m. Statistical significance was determined by two-sided Student's *t*-test.

accumulation experiment; we observed a 60% reduction in intracellular accumulation of [³H]-docetaxel in MMTV-PyVmt;*Abcc10*$^{+/+}$ compared with MMTV-PyVmt;*Abcc10*$^{-/-}$ cell lines (Figure 4D). The amount of reduction in [³H]-docetaxel is comparable to reduction we published using ABCC10 transfectants (Malofeeva *et al*, 2012). Cell cycle analysis showed a marked, dose-dependent G2/M accumulation of MMTV-PyVmt; *Abcc10*$^{-/-}$ mammary tumour cell lines after 48 h of docetaxel exposure (Figure 5A) or paclitaxel (Figure 5B) but no such accumulation for MMTV-PyVmt;*Abcc10*$^{+/+}$ cell lines (Figures 5A and B). A 48-h treatment with 25 nM docetaxel led to a non-statistically significant trend towards early apoptosis in MMTV-PyVmt; *Abcc10*$^{-/-}$ but not MMTV-PyVmt;*Abcc10*$^{+/+}$ cell lines (Figure 5C). Similarly, 25 nM paclitaxel significantly increased

apoptosis in MMTV-PyVmt; *Abcc10*$^{-/-}$ but not in the MMTV-PyVmt;*Abcc10*$^{+/+}$ cell lines (Figure 5D).

ABCC10 loss increased the impact of docetaxel treatment in an orthotopic mammary tumour model. An orthotopic mammary tumour model was used to extend our *in vitro* work to a more clinically relevant *in vivo* model, offering the additional ability to characterise the cell lines *in vitro* and *in vivo*. To determine whether Abcc10 status affects mammary tumour sensitisation to taxanes MMTV-PyVmT; *Abcc10*$^{+/+}$ and MMTV-PyVmT; *Abcc10*$^{-/-}$ mammary tumour-derived cells (three cell lines per genotype) were implanted into the mammary gland area of 8-week-old female mice (*n* = 15 per cell line). Two weeks later, when the tumours grew to ∼50 mm³, the mice were divided into
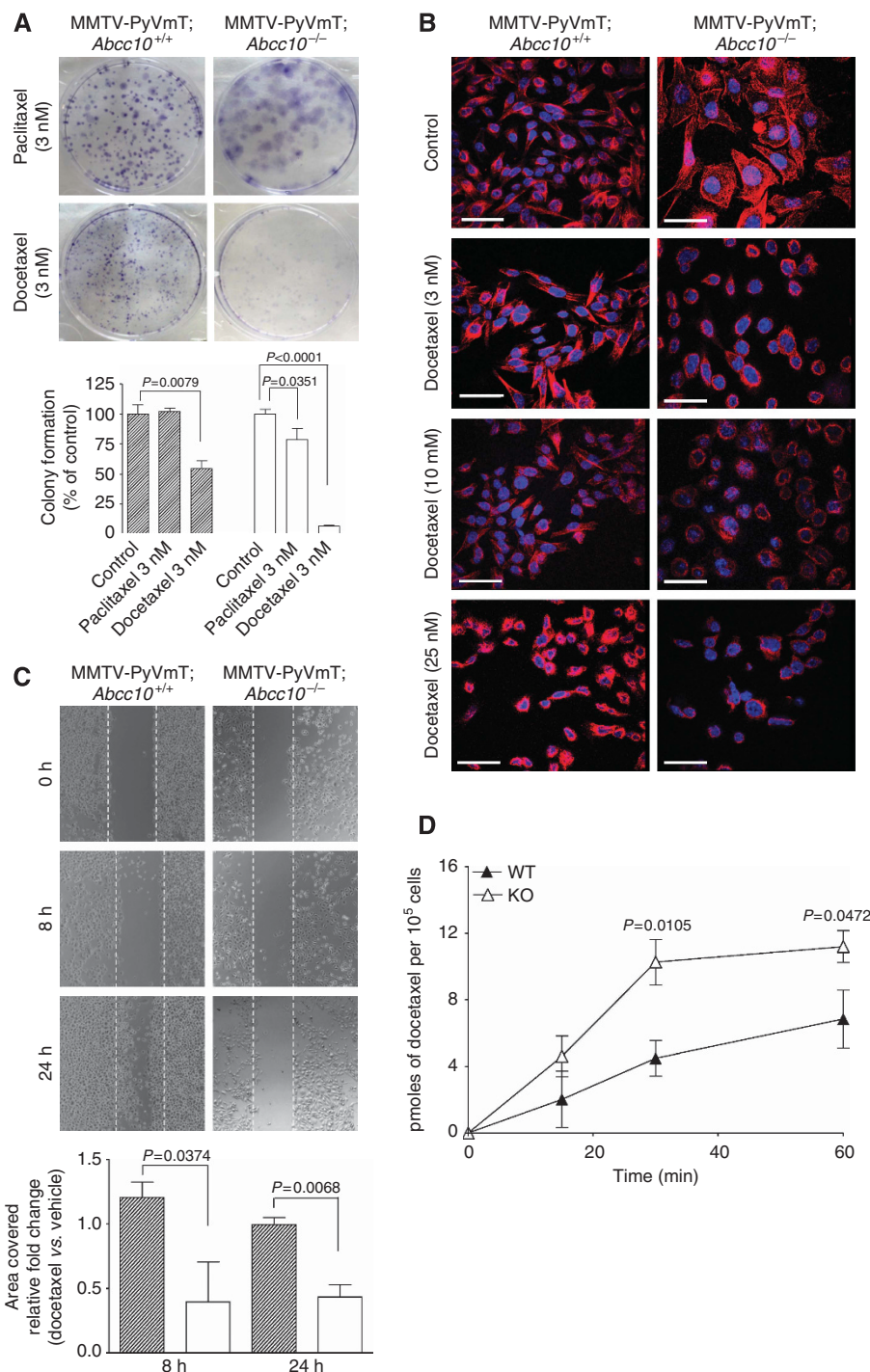
Figure 4. Mammary tumour cell lines originating from PyVmT;Abcc10 null cells are sensitised to cytotoxic ABCC10 substrates. (A) Images of colonies from $Abcc10^{-/-}$ vs $Abcc10^{+/+}$ cells following paclitaxel or docetaxel treatment (the analysis with controls is presented on graphs under images). (B) Microtubule staining of $Abcc10$ wild-type and $Abcc10$ null cell lines after incubation with 3, 10, or 25 nM of docetaxel; tubulin (red), nuclei (blue). Scale bar, 100 μm. (C) Images from wound-healing assays assessing the mobility of wild-type and $Abcc10^{-/-}$ lines after docetaxel treatment (the analysis with controls is presented on graphs under images). (D) Accumulation of 0.1 μM [^{3}H]-docetaxel in $Abcc10^{+/+}$ cells (WT, black triangle) compared with the mammary tumour cell lines derived from $Abcc10$-disrupted mice (KO, white triangle) was observed. Error bars denote mean ± s.e.m. Statistical significance was determined by two-sided Student's t-test.

two groups: a vehicle control group ($n = 5$) and a 25-mg kg^{-1} docetaxel treatment group ($n = 10$). The mice were treated weekly by intraperitoneal injection until the tumours reached 200 mm^3. As in primary tumour formation, MMTV-PyVmT; $Abcc10^{-/-}$ tumours grew more rapidly than did MMTV-PyVmT; $Abcc10^{+/+}$ tumours (Figures 6A; $P = 0.001$). PyVMT; $Abcc10^{+/+}$ and $Abcc10^{-/-}$ tumours were both responsive to docetaxel

($P = 0.003$ and $P < 0.001$). Importantly, over 21 days while MMTV-PyVmT; $Abcc10^{+/+}$ tumour size was reduced by 50%, MMTV-PyVmT; $Abcc10^{-/-}$ tumour sensitisation to docetaxel was more dramatic as tumour size was reduced by 86% compared with untreated mice. To further compare the effectiveness of docetaxel treatment on wild-type and $Abcc10$ knockout tumours, we analysed the impact of Abcc10 status on proliferation
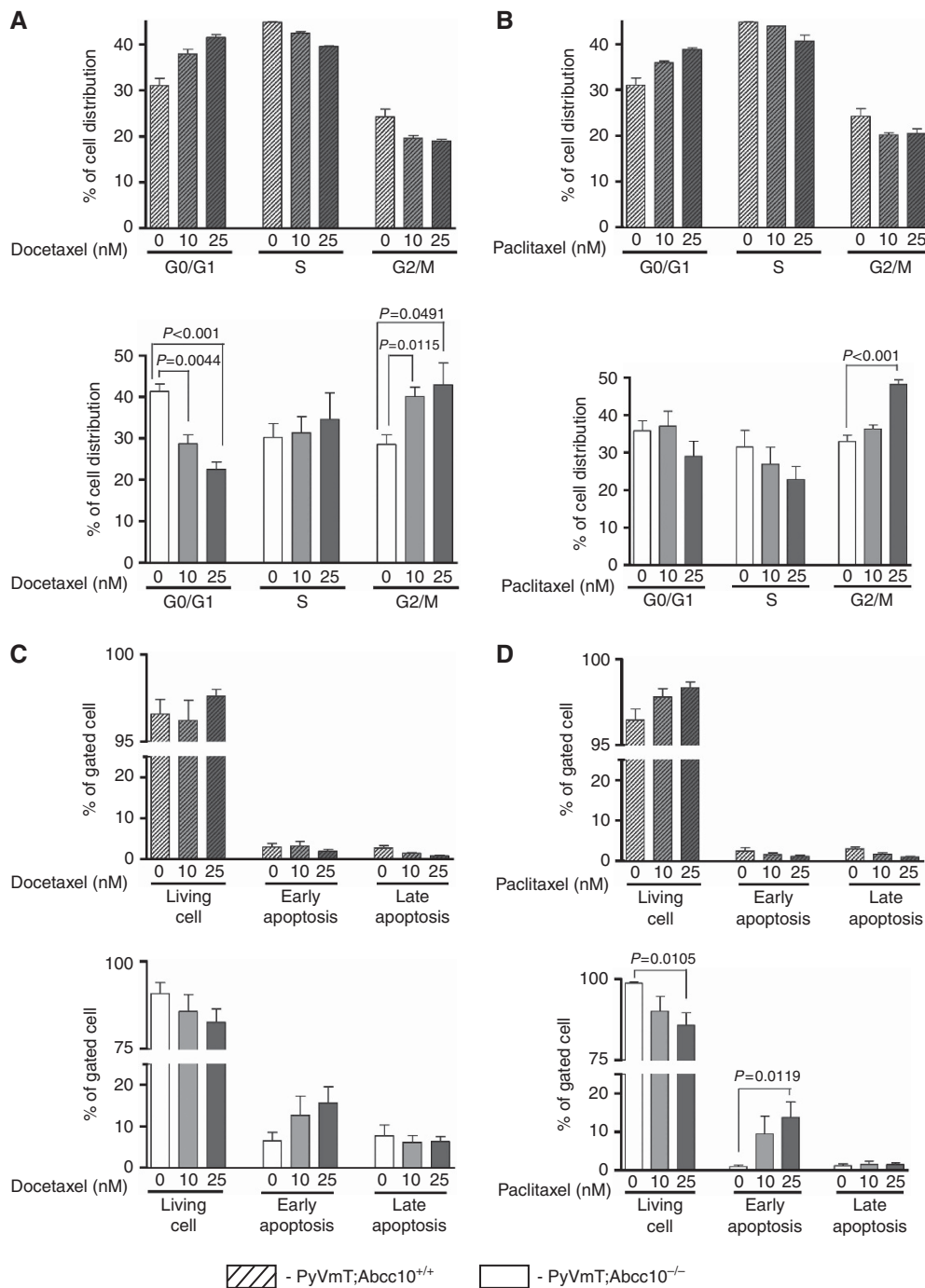
Figure 5. Effects of docetaxel and paclitaxel on cell cycle progression and apoptosis induction in MMTV-PyVT;Abcc10$^{+/+}$ and MMTV-PyVT; Abcc10$^{-/-}$ primary mammary tumours cells. After treatment with 0, 10, or 25 nM docetaxel or paclitaxel, cells were harvested for analysis of cell cycle distribution or apoptosis. Cell cycle distribution is shown after 48 h of docetaxel (A) or paclitaxel (B) treatment. Percentage of living cells, and early and late apoptosis are shown following 48 h of docetaxel (C) or paclitaxel (D) treatment. Shade, MMTV-PyVT;Abcc10$^{+/+}$ cell lines; blank, MMTV-PyVT;Abcc10$^{-/-}$ cell lines. Error bars denote mean ± s.e.m. Statistical significance was determined by two-sided Student's t-test.

rate, vascularisation, and apoptosis after docetaxel treatment. The graph represents the relative fold change (Docetaxel vs Vehicle) where vehicle treated is 1 for both wild-type and Abcc10 knockout tumours. We found that Abcc10$^{-/-}$ tumours showed a significant reduction in Ki-67-positive cells (Figure 6C), as well as a reduction in blood vessel density compared with MMTV-PyVmT; Abcc10$^{+/+}$ after treatment (Figure 6D). We also observed that the number of apoptotic cells in treated Abcc10 knockout tumours was increased more than threefold compared with Abcc10$^{-/-}$ control tumours. Lastly, we saw an increased number of apoptotic

cells in Abcc10$^{-/-}$-treated tumours compared with wild-type treated tumours (Figure 6E).

MMTV-PyVmT;Abcc10$^{-/-}$ mice experienced enhanced docetaxel-dependent therapy and increased overall survival compared with MMTV-PyVmT;Abcc10$^{+/+}$ counterparts. We used the primary MMTV-PyVmT tumour model with Abcc10$^{-/-}$ and Abcc10$^{+/+}$ genotypes to assess the therapeutic effect of docetaxel in vivo. Mice were treated with vehicle or 25 mg kg^{-1} of docetaxel weekly for 12 weeks. Mice were also killed if the largest

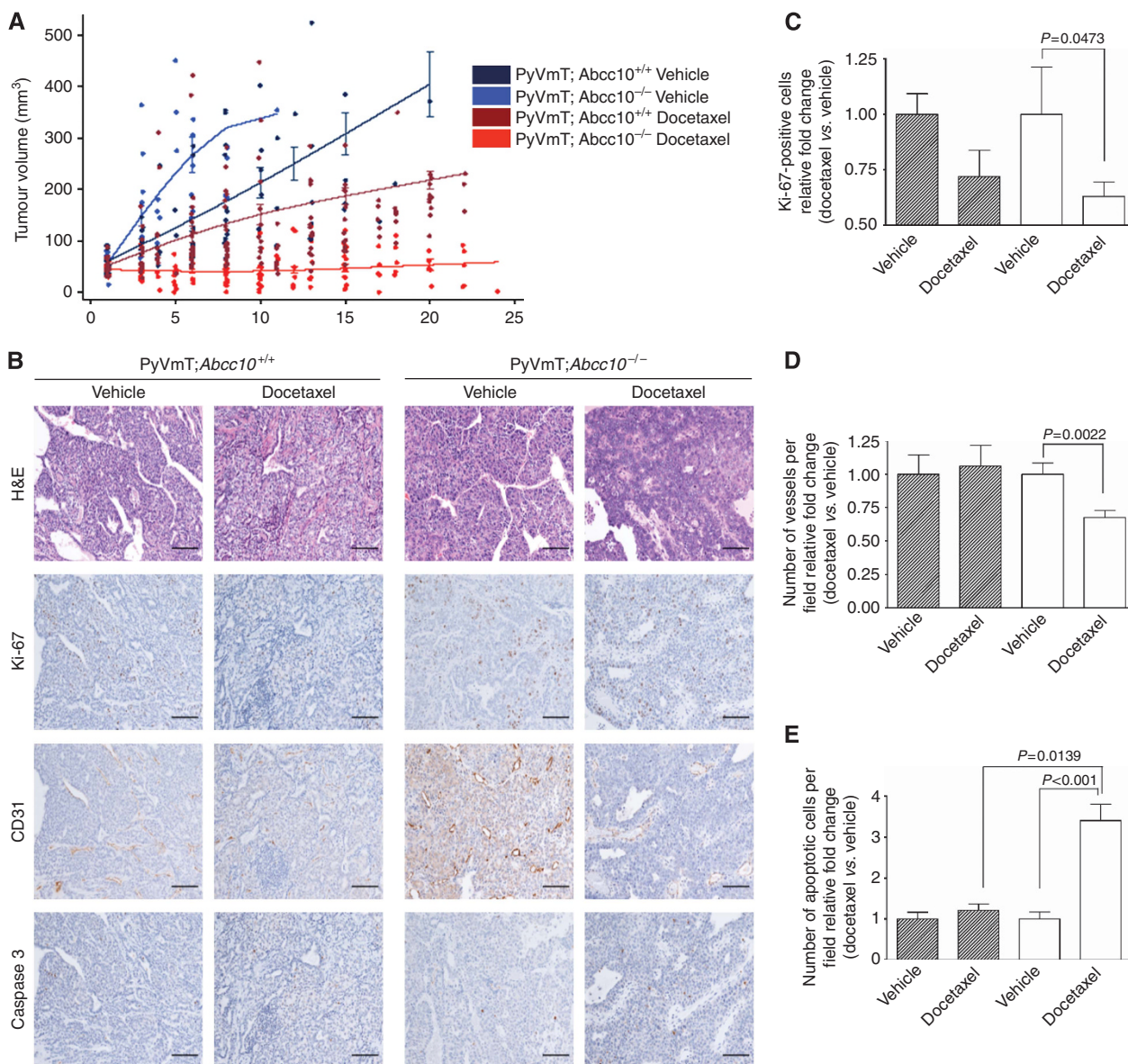Figure 6. Therapeutic effects of docetaxel on orthotopic mammary tumour model. (A) Allograft model of SCID mice injected with Abcc10$^{-/-}$ or wild-type lines treated with docetaxel after tumour development (wild-type: vehicle, grey; docetaxel, brown. Knockout: vehicle, blue; docetaxel, red). (B) Histological and immunohistochemical assessments of Abcc10 wild-type and knockout tumours treated with or without docetaxel at a dosage of 25 mg kg^{-1} (treated n = 4, vehicle n = 2 per genotype). Scale bar, 100 µm. (C–E) Quantification of the following parameters: proliferation by Ki-67 staining (C), blood vessel density by CD31 staining (D), and apoptosis (E) by Caspase 3 staining. Five high-power fields (× 20) were examined per tumour. Error bars denote mean ± s.e.m. Statistical significance was determined by two-sided Student's t-test.

tumour reached 1000 mm^3 or if the total tumour burden was greater than 10% of body weight (Figure 7A and B). MMTV-PyVmT; Abcc10$^{-/-}$ mice were responsive to docetaxel treatment over time (P = 0.006) compared with wild-type mice (P = 0.063; Figure 7B). Treated wild-type mice reached the study end points and died much earlier compared with MMTV-PyVmT; Abcc10$^{-/-}$ mice treated with docetaxel; at 8 weeks only 44% of wild-type mice survived in contrast 100% of Abcc10 knockout mice were still alive. Kaplan–Meier curve analysis indicated significantly increased survival of docetaxel-treated MMTV-PyVmT; Abcc10$^{-/-}$ mice compared with wild-type mice (Figure 7C).

DISCUSSION

In this study, we investigated the impact of ABCC10 loss on breast tumour phenotype and tumour sensitisation using a novel MMTV-PyVmT; Abcc10$^{-/-}$ model. Although they grew more rapidly, tumours derived from MMTV-PyVmT; Abcc10$^{-/-}$ mice had decreased apoptosis, blood vessel formation, and lung metastasis in contrast to those from MMTV-PyVmT; Abcc10$^{+/+}$ mice. This was accompanied by numerous differences in the growth properties of cell lines associated with the two genotypes, including most markedly differences in proliferation and migration. Here we showed that cell lines derived from wild-type tumours were less adherent and were more migratory active compared with cell lines derived from Abcc10 null tumours. These characteristics phenocopy the metastatic properties of tumours in vivo. During metastatic disease, cancer cells leave the primary site (reduced adhesion) and go to the secondary environment (migratory activity). Many studies in experimental model systems and in human patients have revealed that alterations in the adhesive and migratory properties of tumour cells correlate with progression to tumour malignancy (Hirohashi, 1998; Cavallaro and Christofori, 2001).
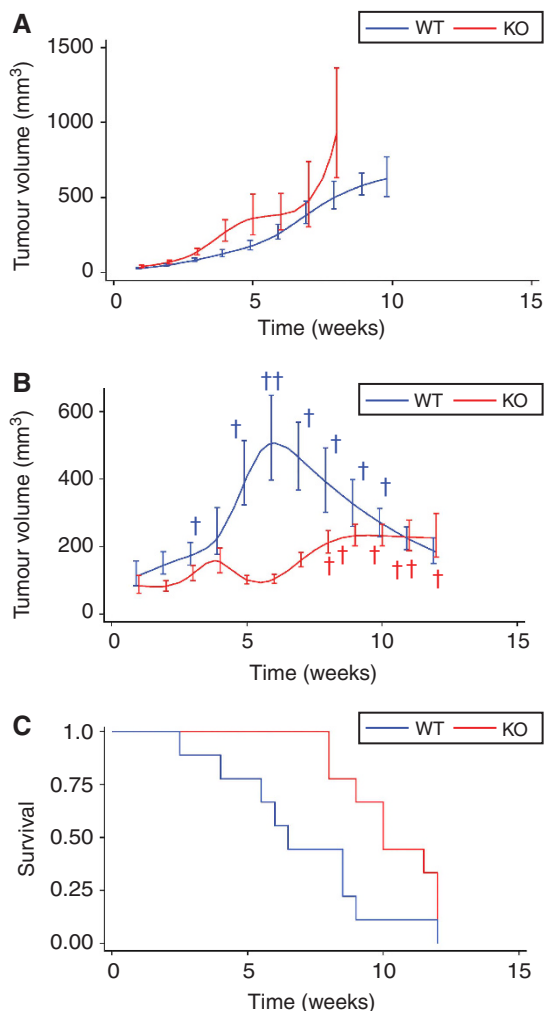
Figure 8. Summary of effects of Abcc10 loss on pathways. Abcc10 loss increased proliferation *in vitro* and *in vivo*, decreased number of lung metastasis in MMTV-PyVmT mammary tumour model, and increased drug sensitivity. ABCC10 may be connected to cellular signalling pathways of proliferation and growth.

Figure 7. Therapeutic effects of docetaxel on MMTV-PyVmT mice with *Abcc10*$^{-/-}$ and *Abcc10*$^{+/+}$ genotypes. (**A**) Comparison of growth rates of MMTV-PyVmT;*Abcc10*$^{-/-}$ (red line; $n = 9$) mammary tumours and MMTV-PyVmT;*Abcc10*$^{+/+}$ tumours treated with vehicle (blue line; $n = 8$). (**B**) Comparison of growth rates of MMTV-PyVmT;*Abcc10*$^{-/-}$ (red line; $n = 9$) mammary tumours and MMTV-PyVmT;*Abcc10*$^{+/+}$ tumours treated with docetaxel (blue line; $n = 9$). †Death. (**C**) Kaplan–Meier curve analysis indicated increased survival of docetaxel-treated MMTV-PyVmT;*Abcc10*$^{-/-}$ mice compared with wild-type docetaxel-treated mice ($P = 0.0298$). Error bars denote mean $\pm$ s.e.m.

Taken together, these data imply that, similar to ABCC1 and ABCC3, ABCC10 has important roles beyond controlling drug efflux in mammary tumour biology. We hypothesise that these phenotypes may be related to ABCC10's ability to transport as yet unidentified physiological substrate(s). Alternatively it is possible that ABCC10 has a role in signalling pathways that mediate processes such as proliferation, malignant transformation, cell survival, and drug resistance. It has been reported previously that inhibition of ABCG2 expression in A549 cells or mixantrone-resistant MCF cells by shRNA inhibited proliferation, cell cycle progression. and also modulated the expression of cell cycle regulator genes (Chen *et al*, 2010). Although the exact mechanisms through which ABCG2 or ABCC10 mediate these processes are unknown, prior studies suggest a link between ABC transporters and MAPK/ERK or PI3K/AKT signalling pathways (Bleau *et al*, 2009; Hoffmann *et al*, 2011; Imai *et al*, 2012; Pick and Wiese, 2012; Huang *et al*, 2013). Figure 8 illustrates a schematic which summarises the effects of ABCC10 loss, as well as potential
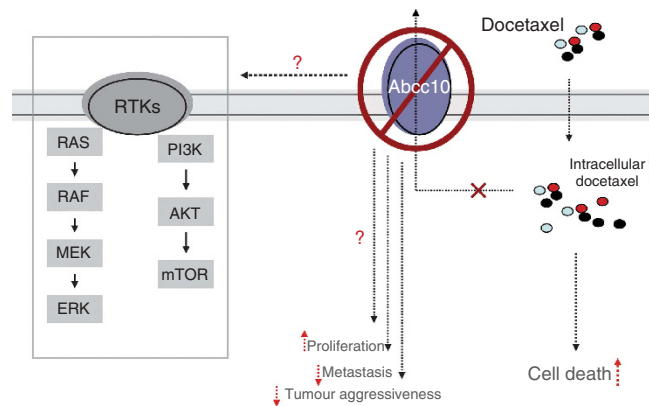
pathways to investigate in connection with ABCC10 expression. Further studies are required to define the exact mechanisms in which ABCC10 is involved; hence, this area is currently under investigation in our laboratory.

Knowledge of ABCC10 expression is important for understanding the potential effects of this pump's activity in normal and malignant tissues. ABCC10 transcript expression is widespread, with highest levels detected in the gonads and spleen (Hopper-Borge *et al*, 2009). The ABCC10 transcript has been detected in multiple types of adenocarcinoma that are routinely treated with taxanes, including breast, ovary, and lung (Dabrowska and Sirotnak, 2004; Takayanagi *et al*, 2004). ABCC10 transcript has also been found in hepatocellular carcinoma (Borel *et al*, 2012) and colorectal tumours (Hlavata *et al*, 2012). Recent work has shown that ABCC10 is among the transporters that are upregulated in pancreatic adenocarcinoma tumours compared with normal tissue and the idea was put forth that ABCC10 might contribute to poor treatment response in this tumour type (Mohelnikova-Duchonova *et al*, 2013). Another paper compared the absolute gene expression of all the human xenobiotic transporter genes in various tissue types and tumours. These authors demonstrated that ABCC10 expression in tumours derived from lung, colon, and breast was relatively high in terms of absolute intensity (Bleasby *et al*, 2006). However, only few studies have been published regarding ABCC10 protein expression. Immunohistochemical staining of normal and tumour tissues revealed that ABCC10 is upregulated in cancer compared with the normal lung (Wang *et al*, 2009). ABCC10 protein expression was also evaluated in two human head and neck cancer cell lines, SCCHA and HSY. ABCC10 was not detected in the parental cell lines. However, after vincristine treatment ABCC10 was upregulated in the HSY cell line (Naramoto *et al*, 2007).

In this report we demonstrate that ABCC10 is expressed in various breast cancer lines and importantly that it is expressed in clinical samples derived from several breast cancer molecular subtypes. Further, we showed that ABCC10 is more highly expressed in HER2 + and ER + human breast cancer cell lines. Analysis of human tumour tissue also showed higher expression of ABCC10 in HER2 + and ER + tumours. Interestingly, the triple-negative breast cancer subtype was more heterogeneous for ABCC10 expression compared with other subtypes. This observation suggests that it may be prudent to investigate ABCC10 as a novel potential target for clinical screening of triple-negative breast cancer as this information could support the development of more personalised therapies. Further, triple-negative breast cancer has

the worst prognosis of the breast cancer subtypes and affects African American women disproportionately (Stead *et al*, 2009). It is of considerable interest to assess ABCC10 protein expression in African American women to determine whether ABCC10 expression is linked to health disparities in response to treatment.

We recently demonstrated that ABCC10 transporter activity is inhibited by sorafenib, a multitargeted tyrosine kinase inhibitor currently in use for the treatment of renal cell carcinoma and other cancers (Malofeeva *et al*, 2012). At this time, there are no identified inhibitors with specific, *in vivo* efficacy against endogenous ABCC10; an important goal for future work would be the exploration of the ability of sorafenib, cepharanthine, and other putative inhibitors to modulate *in vivo* taxane transport capabilities of ABCC10 in relevant preclinical models. ABCC10 inhibition is particularly nominated as a potentially high-value target for inhibition based on its physiological relevance to *in vivo* taxane resistance in breast cancer. Whether absence of ABCC10 sensitises solid tumours to taxanes while not leading to unacceptable toxicity in normal tissue remains to be determined (Burkhart *et al*, 2009). In summary, we showed that ABCC10 does not only modulate drug transport but has an impact on tumour biology. For better understanding of the mechanisms by which Abcc10 influences proliferation, migration, and metastasis, further investigation will be required. Importantly, we also showed that elimination of endogenous Abcc10 has a profound effect on tumour sensitization to taxanes and overall survival. This work emphasises the value of future studies of ABCC10 in breast cancer pathogenesis and resistance to treatment.

ACKNOWLEDGEMENTS

CONFLICT OF INTEREST

The authors declare no conflict of interest.

REFERENCES

Amiri-Kordestani L, Basseville A, Kurdziel K, Fojo AT, Bates SE (2013) Targeting MDR in breast and lung cancer: discriminating its potential importance from the failure of drug resistance reversal studies. *Drug Resist Updat* **15**(1–2): 50–61.

Bleasby K, Castle JC, Roberts CJ, Cheng C, Bailey WJ, Sina JF, Kulkarni AV, Hafey MJ, Evers R, Johnson JM, Ulrich RG, Slatter JG (2006) Expression profiles of 50 xenobiotic transporter genes in humans and pre-clinical species: a resource for investigations into drug disposition. *Xenobiotica* **36**(10–11): 963–988.

Bleau AM, Hambardzumyan D, Ozawa T, Fomchenko EI, Huse JT, Brennan CW, Holland EC (2009) PTEN/PI3K/Akt pathway regulates the side population phenotype and ABCG2 activity in glioma tumor stem-like cells. *Cell Stem Cell* **4**(3): 226–235.

Bolstad BM, Irizarry RA, Astrand M, Speed TP (2003) A comparison of normalization methods for high density oligonucleotide array data based on variance and bias. *Bioinformatics* **19**(2): 185–193.

Borel F, Han R, Visser A, Petry H, van Deventer SJ, Jansen PL, Konstantinova P. Reseau Centre de Ressources Biologiques Foie F (2012) Adenosine triphosphate-binding cassette transporter genes up-regulation in untreated hepatocellular carcinoma is mediated by cellular microRNAs. *Hepatology* **55**(3): 821–832.

Burkhart CA, Watt F, Murray J, Pajic M, Prokvolit A, Xue C, Flemming C, Smith J, Purmal A, Isachenko N, Komarov PG, Gurova KV, Sartorelli AC, Marshall GM, Norris MD, Gudkov AV, Haber M (2009) Small-molecule multidrug resistance-associated protein 1 inhibitor reversan increases the therapeutic index of chemotherapy in mouse models of neuroblastoma. *Cancer Res* **69**(16): 6573–6580.

Cai KQ, Wu H, Klein-Szanto AJ, Xu XX (2009) Acquisition of a second mutation of the Tp53 alleles immediately precedes epithelial morphological transformation in ovarian tumorigenicity. *Gynecol Oncol* **114**(1): 18–25.

Cavallaro U, Christofori G (2001) Cell adhesion in tumor invasion and metastasis: loss of the glue is not enough. *Biochim Biophys Acta* **1552**(1): 39–45.

Chen Z, Liu F, Ren Q, Zhao Q, Ren H, Lu S, Zhang L, Han Z (2010) Suppression of ABCG2 inhibits cancer cell proliferation. *Int J Cancer* **126**(4): 841–851.

Dabrowska M, Sirotnak FM (2004) Regulation of transcription of the human MRP7 gene. Characteristics of the basal promoter and identification of tumor-derived transcripts encoding additional 5′ end heterogeneity. *Gene* **341**: 129–139.

Dave B, Mittal V, Tan NM, Chang JC (2012) Epithelial-mesenchymal transition, cancer stem cells and treatment resistance. *Breast Cancer Res* **14**(1): 202.

Forrester E, Chytil A, Bierie B, Aakre M, Gorska AE, Sharif-Afshar AR, Muller WJ, Moses HL (2005) Effect of conditional knockout of the type II TGF-beta receptor gene in mammary epithelia on mammary gland development and polyomavirus middle T antigen induced tumor formation and metastasis. *Cancer Res* **65**(6): 2296–2302.

Glavinas H, Krajcsi P, Cserepes J, Sarkadi B (2004) The role of ABC transporters in drug resistance, metabolism and toxicity. *Curr Drug Deliv* **1**(1): 27–42.

Grassilli E, Narloch R, Federzoni E, Ianzano L, Pisano F, Giovannoni R, Romano G, Masiero L, Leone BE, Bonin S, Donada M, Stanta G, Helin K, Lavitrano M (2013) Inhibition of GSK3B Bypass drug resistance of p53-Null colon carcinomas by enabling necroptosis in response to chemotherapy. *Clin Cancer Res* **19**(14): 3820–3831.

Guy CT, Webster MA, Schaller M, Parsons TJ, Cardiff RD, Muller WJ (1992) Expression of the neu protooncogene in the mammary epithelium of transgenic mice induces metastatic disease. *Proc Natl Acad Sci USA* **89**(22): 10578–10582.

Harrell FE (2001) *Regression Modeling Strategies*. In Chapter 2, pp 11–40. Springer: New York, NY.

Henderson MJ, Haber M, Porro A, Munoz MA, Iraci N, Xue C, Murray J, Flemming CL, Smith J, Fletcher JI, Gherardi S, Kwek CK, Russell AJ, Valli E, London WB, Buxton AB, Ashton LJ, Sartorelli AC, Cohn SL, Schwab M, Marshall GM, Perini G, Norris MD (2011) ABCC multidrug transporters in childhood neuroblastoma: clinical and biological effects independent of cytotoxic drug efflux. *J Natl Cancer Inst* **103**(16): 1236–1251.

Higgins MJ, Baselga J (2011) Targeted therapies for breast cancer. *J Clin Invest* **121**(10): 3797–3803.

Hirohashi S (1998) Inactivation of the E-cadherin-mediated cell adhesion system in human cancers. *Am J Pathol* **153**(2): 333–339.

Hlavac V, Brynychova V, Vaclavikova R, Ehrlichova M, Vrana D, Pecha V, Kozevnikovova R, Trnkova M, Gatek J, Kopperova D, Gut I, Soucek P (2013) The expression profile of ATP-binding cassette transporter genes in breast carcinoma. *Pharmacogenomics* **14**(5): 515–529.

Hlavata I, Mohelnikova-Duchonova B, Vaclavikova R, Liska V, Pitule P, Novak P, Bruha J, Vycital O, Holubec L, Treska V, Vodicka P, Soucek P (2012) The role of ABC transporters in progression and clinical outcome of colorectal cancer. *Mutagenesis* **27**(2): 187–196.

Hoffmann K, Shibo L, Xiao Z, Longerich T, Buchler MW, Schemmer P (2011) Correlation of gene expression of ATP-binding cassette protein and tyrosine kinase signaling pathway in patients with hepatocellular carcinoma. *Anticancer Res* **31**(11): 3883–3890.

Hopper-Borge E, Chen ZS, Shchaveleva I, Belinsky MG, Kruh GD (2004) Analysis of the drug resistance profile of multidrug resistance protein 7 (ABCC10): resistance to docetaxel. *Cancer Res* **64**(14): 4927–4930.

Hopper-Borge E, Xu X, Shen T, Shi Z, Chen ZS, Kruh GD (2009) Human multidrug resistance protein 7 (ABCC10) is a resistance factor for nucleoside analogues and epothilone B. *Cancer Res* **69**(1): 178–184.

Hopper-Borge EA, Churchill T, Paulose C, Nicolas E, Jacobs JD, Ngo O, Kuang Y, Grinberg A, Westphal H, Chen ZS, Klein-Szanto AJ, Belinsky MG, Kruh GD (2011) Contribution of Abcc10 (Mrp7) to *in vivo* paclitaxel resistance as assessed in Abcc10 (− / −) mice. *Cancer Res* **71**(10): 3649–3657.

Hopper E, Belinsky MG, Zeng H, Tosolini A, Testa JR, Kruh GD (2001) Analysis of the structure and expression pattern of MRP7 (ABCC10), a new member of the MRP subfamily. *Cancer Lett* **162**(2): 181–191.

Huang FF, Wu DS, Zhang L, Yu YH, Yuan XY, Li WJ, Chen XP, Zhao XL, Chen FP, Zeng H (2013) Inactivation of PTEN increases ABCG2 expression and the side population through the PI3K/Akt pathway in adult acute leukemia. *Cancer Lett* **336**(1): 96–105.

Huisman MT, Chhatta AA, van Tellingen O, Beijnen JH, Schinkel AH (2005) MRP2 (ABCC2) transports taxanes and confers paclitaxel resistance and both processes are stimulated by probenecid. *Int J Cancer* **116**(5): 824–829.

Imai Y, Yamagishi H, Ono Y, Ueda Y (2012) Versatile inhibitory effects of the flavonoid-derived PI3K/Akt inhibitor, LY294002, on ATP-binding cassette transporters that characterize stem cells. *Clin Transl Med* **1**(1): 24.

Ishihara D, Dovas A, Hernandez L, Pozzuto M, Wyckoff J, Segall JE, Condeelis JS, Bresnick AR, Cox D (2013) Wiskott-Aldrich syndrome protein regulates leukocyte-dependent breast cancer metastasis. *Cell Rep* **4**(3): 429–436.

Izumchenko E, Singh MK, Plotnikova OV, Tikhmyanova N, Little JL, Serebriiskii IG, Seo S, Kurokawa M, Egleston BL, Klein-Szanto A, Pugacheva EN, Hardy RR, Wolfson M, Connolly DC, Golemis EA (2009) NEDD9 promotes oncogenic signaling in mammary tumor development. *Cancer Res* **69**(18): 7198–7206.

Kelly RJ, Robey RW, Chen CC, Draper D, Luchenko V, Barnett D, Oldham RK, Caluag Z, Frye AR, Steinberg SM, Fojo T, Bates SE (2012) A pharmacodynamic study of the P-glycoprotein antagonist CBT-1(R) in combination with paclitaxel in solid tumors. *Oncologist* **17**(4): 512.

Keppler D (2011) Multidrug resistance proteins (MRPs, ABCCs): importance for pathophysiology and drug therapy. *Handb Exp Pharmacol* **201**: 299–323.

Kononen J, Bubendorf L, Kallioniemi A, Barlund M, Schraml P, Leighton S, Torhorst J, Mihatsch MJ, Sauter G, Kallioniemi OP (1998) Tissue microarrays for high-throughput molecular profiling of tumor specimens. *Nat Med* **4**(7): 844–847.

Kuo PL, Hsu YL, Cho CY (2006) Plumbagin induces G2-M arrest and autophagy by inhibiting the AKT/mammalian target of rapamycin pathway in breast cancer cells. *Mol Cancer Ther* **5**(12): 3209–3221.

Lin EY, Jones JG, Li P, Zhu L, Whitney KD, Muller WJ, Pollard JW (2003) Progression to malignancy in the polyoma middle T oncoprotein mouse breast cancer model provides a reliable model for human diseases. *Am J Pathol* **163**(5): 2113–2126.

Malofeeva E, Domanitskaya N, Gudima M, Hopper-Borge EA (2012) Modulation of the ATPase and transport activities of broad-acting multidrug resistance factor ABCC10 (MRP7). *Cancer Res* **72**(24): 6457–6467.

Marcotte R, Smith HW, Sanguin-Gendreau V, McDonough RV, Muller WJ (2012) Mammary epithelial-specific disruption of c-Src impairs cell cycle progression and tumorigenesis. *Proc Natl Acad Sci USA* **109**(8): 2808–2813.

McMillin DW, Negri JM, Mitsiades CS (2013) The role of tumour-stromal interactions in modifying drug response: challenges and opportunities. *Nat Rev Drug Discov* **12**(3): 217–228.

Mohelnikova-Duchonova B, Brynychova V, Oliverius M, Honsova E, Kala Z, Muckova K, Soucek P (2013) Differences in transcript levels of ABC transporters between pancreatic adenocarcinoma and nonneoplastic tissues. *Pancreas* **42**(4): 707–716.

Naramoto H, Uematsu T, Uchihashi T, Doto R, Matsuura T, Usui Y, Uematsu S, Li X, Takahashi M, Yamaoka M, Furusawa K (2007) Multidrug resistance-associated protein 7 expression is involved in cross-resistance to docetaxel in salivary gland adenocarcinoma cell lines. *Int J Oncol* **30**(2): 393–401.

O'Donovan N, Crown J, Stunell H, Hill AD, McDermott E, O'Higgins N, Duffy MJ (2003) Caspase 3 in breast cancer. *Clin Cancer Res* **9**(2): 738–742.

Oguri T, Ozasa H, Uemura T, Bessho Y, Miyazaki M, Maeno K, Maeda H, Sato S, Ueda R (2008) MRP7/ABCC10 expression is a predictive biomarker for the resistance to paclitaxel in non-small cell lung cancer. *Mol Cancer Ther* **7**(5): 1150–1155.

Parsons M, Heike G (2009) How to make tissue microarrays. *Diagn Histopathol* **15**(3): 142–149.

Pick A, Wiese M (2012) Tyrosine kinase inhibitors influence ABCG2 expression in EGFR-positive MDCK BCRP cells via the PI3K/Akt signaling pathway. *ChemMedChem* **7**(4): 650–662.

Shults J, Ratcliffe SJ, Leonard M (2007) Improved generalized estimating equation analysis via xtqls for implementation of quasi-least squares in Stata. *Strata J* **7**(2): 147–166.

Smyth GK (2004) Linear models and empirical bayes methods for assessing differential expression in microarray experiments. *Stat Appl Genet Mol Biol* **3**: Article 3.

Soerjomataram I, Louwman MW, Ribot JG, Roukema JA, Coebergh JW (2008) An overview of prognostic factors for long-term survivors of breast cancer. *Breast Cancer Res Treat* **107**(3): 309–330.

Stead LA, Lash TL, Sobieraj JE, Chi DD, Westrup JL, Charlot M, Blanchard RA, Lee JC, King TC, Rosenberg CL (2009) Triple-negative breast cancers are increased in black women regardless of age or body mass index. *Breast Cancer Res* **11**(2): R18.

Sui M, Huang Y, Park BH, Davidson NE, Fan W (2007) Estrogen receptor alpha mediates breast cancer cell resistance to paclitaxel through inhibition of apoptotic cell death. *Cancer Res* **67**(11): 5337–5344.

Szakacs G, Annereau JP, Lababidi S, Shankavaram U, Arciello A, Bussey KJ, Reinhold W, Guo Y, Kruh GD, Reimers M, Weinstein JN, Gottesman MM (2004) Predicting drug sensitivity and resistance: profiling ABC transporter genes in cancer cells. *Cancer Cell* **6**(2): 129–137.

Takayanagi S, Kataoka T, Ohara O, Oishi M, Kuo MT, Ishikawa T (2004) Human ATP-binding cassette transporter ABCC10: expression profile and p53-dependent upregulation. *J Exp Ther Oncol* **4**(3): 239–246.

Ueno NT, Yu D, Hung MC (1997) Chemosensitization of HER-2/neu-overexpressing human breast cancer cells to paclitaxel (Taxol) by adenovirus type 5 E1A. *Oncogene* **15**(8): 953–960.

Wang P, Zhang Z, Gao K, Deng Y, Zhao J, Liu B, Li X (2009) Expression and clinical significance of ABCC10 in the patients with non-small cell lung cancer.. *Zhongguo Fei Ai Za Zhi* **12**(8): 875–878.

Woodward EJ, Twelves C (2010) Scheduling of taxanes: a review. *Curr Clin Pharmacol* **5**(3): 226–231.

Yamada A, Ishikawa T, Ota I, Kimura M, Shimizu D, Tanabe M, Chishima T, Sasaki T, Ichikawa Y, Morita S, Yoshiura K, Takabe K, Endo I (2013) High expression of ATP-binding cassette transporter ABCC11 in breast tumors is associated with aggressive subtypes and low disease-free survival. *Breast Cancer Res Treat* **137**(3): 773–782.

Supplementary Information accompanies this paper on British Journal of Cancer website (http://www.nature.com/bjc)